

Cytoneme-Mediated Delivery of Hedgehog Regulates the Expression of Bone Morphogenetic Proteins to Maintain Germline Stem Cells in *Drosophila*

Patricia Rojas-Ríos¹, Isabel Guerrero², Acaimo González-Reyes^{1*}

1 Centro Andaluz de Biología del Desarrollo, CSIC/Universidad Pablo de Olavide, Sevilla, Spain, **2** Centro de Biología Molecular Severo Ochoa, CSIC/Universidad Autónoma de Madrid, Madrid, Spain

Abstract

Stem cells reside in specialised microenvironments, or niches, which often contain support cells that control stem cell maintenance and proliferation. Hedgehog (Hh) proteins mediate homeostasis in several adult niches, but a detailed understanding of Hh signalling in stem cell regulation is lacking. Studying the *Drosophila* female germline stem cell (GSC) niche, we show that Hh acts as a critical juxtacrine signal to maintain the normal GSC population of the ovary. Hh production in cap cells, a type of niche support cells, is regulated by the Engrailed transcription factor. Hh is then secreted to a second, adjacent population of niche cells, the escort cells, where it activates transcription of the GSC essential factors Decapentaplegic (Dpp) and Glass bottom boat (Gbb). In wild-type niches, Hh protein decorates short filopodia that originate in the support cap cells and that are functionally relevant, as they are required to transduce the Hh pathway in the escort cells and to maintain a normal population of GSCs. These filopodia, reminiscent of wing disc cytonemes, grow several fold in length if Hh signalling is impaired within the niche. Because these long cytonemes project directionally towards the signalling-deficient region, cap cells sense and react to the strength of Hh pathway transduction in the niche. Thus, the GSC niche responds to insufficient Hh signalling by increasing the range of Hh spreading. Although the signal(s) perceived by the cap cells and the receptor(s) involved are still unknown, our results emphasise the integration of signals necessary to maintain a functional niche and the plasticity of cellular niches to respond to challenging physiological conditions.

Citation: Rojas-Ríos P, Guerrero I, González-Reyes A (2012) Cytoneme-Mediated Delivery of Hedgehog Regulates the Expression of Bone Morphogenetic Proteins to Maintain Germline Stem Cells in *Drosophila*. PLoS Biol 10(4): e1001298. doi:10.1371/journal.pbio.1001298

Academic Editor: Thomas Kornberg, University of California, San Francisco, United States of America

Received: July 12, 2011; **Accepted:** February 17, 2012; **Published:** April 3, 2012

Copyright: © 2012 Rojas-Ríos et al. This is an open-access article distributed under the terms of the Creative Commons Attribution License, which permits unrestricted use, distribution, and reproduction in any medium, provided the original author and source are credited.

Funding: This work was supported by the Spanish Ministerio de Ciencia e Innovación and the FEDER programme (grants BFU2006-10934 and BFU2009-08013 to A.G.-R. and BFU2005-04183 and BFU2008-03320 to I. G., and the CONSOLIDER programme CSD-2007-00008), the EU (Marie Curie RTN FP6 (RTN 035528-2) and FP7 (ITN 238186) to I. G.) and by the Junta de Andalucía (Proyectos de Excelencia P06-CVI-01592 and P09-CVI-5058 to A.G.-R.). P.R.-R. was funded by an I3P-CSIC studentship and by the CONSOLIDER programme. The funders had no role in study design, data collection and analysis, decision to publish, or preparation of the manuscript.

Competing Interests: The authors have declared that no competing interests exist.

Abbreviations: BMP, Bone Morphogenetic Protein; CpC, cap cell; Dia, Diaphanus; *disp*, *dispatched*; Dpp, Decapentaplegic; DSHB, Developmental Studies Hybridoma Bank; EC, escort cell; En, Engrailed; Gbb, Glass bottom boat; GSC, germline stem cell; Hh, Hedgehog; Jak/Stat, Janus kinase/Signal transducer and activator of transcription; PBT, PBS containing 0.1% Tween-20; Ptc, Patched; s.d., standard deviation; Smo, Smoothed; TFC, terminal filament cell

* E-mail: agonrey@upo.es

Introduction

Stem cells are responsible for the integrity of tissues during growth, ageing, and repair. They reside in specialised microenvironments, or niches, which frequently comprise support cells that control stem cell self-renewal, proliferation, and differentiation [1,2]. Stem cell niche regulation often involves short-range signalling between stem cells themselves and the surrounding microenvironment. One such short-range signal is the Hedgehog (Hh) family of proteins, which mediates homeostasis in several adult tissues, including the gastrointestinal tract, the hematopoietic system, and the vertebrate central nervous system [3–7]. In fact, Hh signalling dysfunction can lead to stem cell depletion or proliferative disorders such as tumorigenesis [8,9]. However, the detailed mechanisms by which Hh acts in stem cell maintenance remain elusive.

In *Drosophila* females, germline stem cells (GSCs) are located at the apex of the ovary, in a structure termed the germarium that

constitutes a well-defined stem cell niche. The germarium hosts three types of somatic niche cells: terminal filament cells (TFCs), cap cells (CpCs), and escort cells (ECs), which support two to three GSCs and which can be labelled with specific markers such as the *bab1-Gal4* and *patched-Gal4* drivers (Figure 1) [10]. The spatial organisation of the GSC niche permits direct contact between two to three CpCs and one GSC, which is anchored to the CpCs by adherens junctions [11]. In addition, approximately two ECs almost completely surround a given GSC [12]. The coordinated action of GSCs and their support cells allows continuous egg production during adulthood. Thus, GSCs normally divide asymmetrically to produce a differentiating cystoblast and a lineage-renewing GSC daughter [13]. Cystoblasts divide four times to give rise to 2-, 4-, 8-, and 16-cell cysts. ECs transfer the differentiating germline cystoblasts and cysts down the germarium using dynamic cytoplasmic processes [14,15]. Germline cells in the germarium contain specialised organelles rich in membrane skeletal proteins that adopt a spherical (called spectrosome)

Author Summary

The *Drosophila* ovary contains a well-defined stem cell niche that hosts 2–3 germline stem cells (GSCs). The Hedgehog (Hh) family of signalling proteins mediates cellular homeostasis in several adult tissues, and here we decipher the detailed mechanism of action of Hh in the adult female GSC niche. We demonstrate that Hh acts in a juxtacrine manner (i.e., it requires physical contact between the cells involved) to maintain the normal pool of GSCs in the ovarian niche. Hh is produced in one type of niche support cell (the cap cells), and it is received, upon secretion, by a second, neighbouring population of niche cells (the escort cells). In the latter, we show that the Hh signalling pathway regulates the expression of the *Drosophila* Bone Morphogenetic Protein (BMP) homologues and essential stem cell factors *decapentaplegic* (*dpp*) and *glass bottom boat* (*gbb*). We also find that Hh distribution in the GSC niche is mediated by short cellular projections, reminiscent of wing disc cytonemes, although they grow from the (Hh) signal-producing cells towards the receiving cells. Under conditions of low levels of Hh protein and/or Hh signalling within the niche, cap cells emit up to 6-fold longer Hh-decorated cytonemes towards the signalling-deficient area of the niche. Our data reveal that stem cell niches are dynamic structures that can sense, and react to, changes in the activity of essential stem cell factors to prevent stem cell differentiation.

appearance in GSCs and cystoblasts. Upon germline differentiation, the spectrosome grows in size and becomes a branched structure, termed fusome, characteristic of differentiating cysts. Hence, GSCs can be unambiguously identified by their location within the niche (in direct contact with CpCs) and by the presence of spectroosomes (Figure 1).

Reciprocal crosstalk between GSCs and support cells shapes the niche. Firstly, the size and organisation of the CpC cluster depends on proper Notch signalling between GSCs and CpCs [16]. Secondly, both the CpCs and the adjacent ECs play an important role in GSC maintenance, as they transduce the Janus kinase/Signal transducer and activator of transcription (Jak/Stat) pathway to induce the production of the Bone Morphogenetic Protein (BMP) protein Decapentaplegic (Dpp) [12,17,18]. Thirdly, the germline lineage activates the epidermal growth factor receptor pathway in the ECs to repress *dally* expression, thus limiting Dpp movement and stability [19]. Because Dpp (and another BMP homologue called Glass bottom boat [Gbb]) [20,21] act directly on GSCs to repress differentiation and promote self-renewal [22,23], the control of BMP activity is of the utmost importance for correct GSC niche homeostasis.

Here, we demonstrate a key role for the Hh pathway in the regulation of BMP signalling in the *Drosophila* female GSC niche. In addition, we found that wild-type niche support cells grow short Hh-coated filopodia that are functionally relevant for GSC maintenance. Furthermore, support cells sense dysfunctional Hh signalling within the niche and react by growing up to 6-fold longer cytonemes that help increase the range of Hh ligand spreading.

Results

engrailed Is Required Specifically in CpCs for GSC Maintenance

In a number of tissues, the Engrailed (En) transcription factor regulates *hh* expression. Because both *en* and *hh* are expressed in

TFCs and CpCs (Figure 1B and 1C), and considering the importance of the Hh signalling cascade in stem cell maintenance in insects and vertebrates [24,25], we tested whether the *en/hh* connection played a role in the GSC niche. To generate *en*-deficient germlaria, we cultured adult females bearing a thermo-sensitive *en* allele (*en^{SP5}*) in combination with an *en* deficiency (*en^E*) for 7 or 14 d at restrictive temperature (28°C; hereafter referred to as *en^{ts}* germlaria). Compared to control germlaria (*en^{SP5}/CyO*), which contained an average of 2.3±0.8 GSCs and 10.2±1.3 developing cysts (*n*=62; 7 d) and 2.1±0.9 GSCs and 9.1±3.1 developing cysts (*n*=49; 14 d), *en^{ts}* germlaria showed a significant decrease in the average number of GSCs and cysts (1.4±1.1 GSCs and 4.3±2.9 developing cysts, *n*=52, 7 d; 1.2±0.8 GSCs and 3.9±2.5 developing cysts, *n*=41, 14 d). Interestingly, 28.6% of *en^{ts}* germlaria analysed after 7 d at restrictive temperature were devoid of germline cells, which emphasised the importance of *en* gene function in GSC maintenance (Figure 2A–2D; Table S1). To distinguish between a requirement for *en* in the germline versus in the niche support cells, we abolished *en* function from either GSCs or niche cells by utilising two genetically null alleles, *en^E* and *en⁵⁴*. The removal of *en* from the germline did not affect oogenesis, even 3 wk after gene inactivation (*n*>30 for each genotype; Figure 2E). To eliminate the activity of *en* in TFs, CpCs, or ECs we utilised the *bab1-Gal4* driver (Figure 1D). Similar to the removal of *en* from the germline, elimination of *en* from all ECs in contact with a given GSC did not yield a visible phenotype (100% of cases, *n*=23; Figure 2F). However, in 67.7% (*n*=37) of mosaic germlaria where *en* function was removed from at least three clustered CpCs, we observed differentiating cysts that contained branched fusomes and showed the accumulation of the differentiation marker Orb in contact with CpCs (Figures 2G and S1), a phenotype never found in wild-type germlaria. Because we did not detect increased apoptosis in mosaic germlaria containing *en* mutant CpCs and since these mutant cells still expressed CpC markers (Figures S1 and S2), we conclude that *en* is required in CpCs to prevent GSC differentiation.

Hh Release from CpCs Is Required for GSC Maintenance

The effect on the germline of removal of En from CpCs suggested the existence of one or more En-dependent niche cell signals that act on GSCs to promote their maintenance. Hh expression in TFCs and CpCs has been shown to be required for germline development [26] (Figures 1 and S3), which made Hh an excellent candidate to mediate En function in GSC maintenance. We examined the distribution of Hh in mosaic germlaria that contained *en* mutant cells and found that *en* was required in a cell-autonomous fashion for strong membrane accumulation of Hh in TFCs and CpCs (81.8% of mutant cells, *n*=98; Figure 3A and 3B). In addition, we established that the removal of Hh from at least three adjacent CpCs induced GSC differentiation (51.3% of cases, *n*=39; Figure 3C). It has been shown that the release of the cholesterol-modified form of Hh requires the activity of the *dispatched* (*disp*) gene [27]. Interestingly, we found that the removal of *disp* from CpCs was also associated with the appearance of differentiating cysts within the mosaic niche, albeit at a lower frequency (31.6% of germlaria with clusters of ≥3 mutant CpCs, *n*=19; Figure 3D).

The incomplete penetrance of GSC differentiation in *en* and particularly in *hh* or *disp* mosaic niches was most likely due to non-autonomous Hh release from the remaining wild-type cells present in the niche. In fact, the larger the number of *hh* mutant CpCs, the fewer GSCs remained in the niche (see below and Table S2). Alternatively (or in addition), *disp* mutant CpCs may still be able to sustain a certain level of Hh signalling to adjacent ECs, as shown

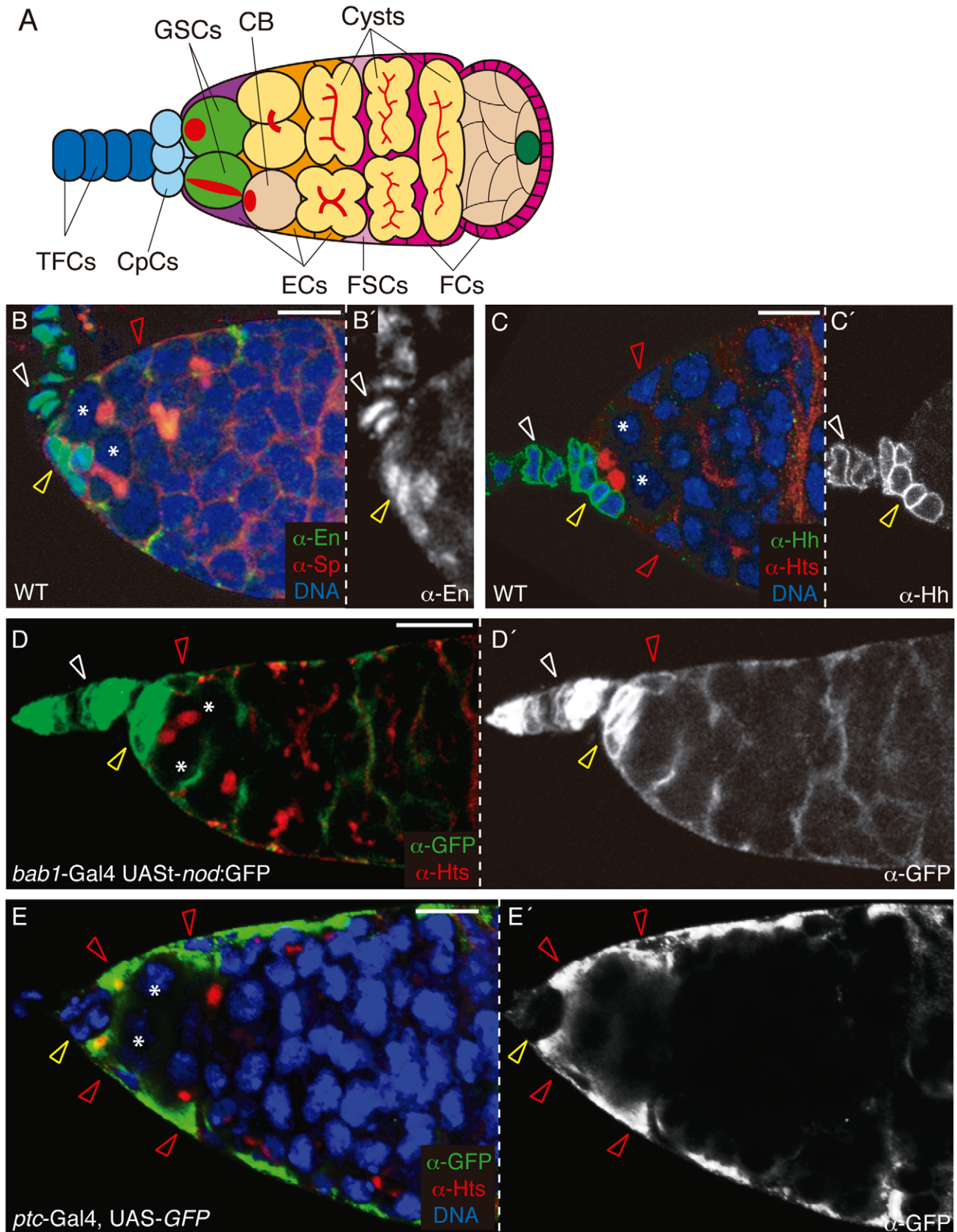


Figure 1. *en* and *hh* are expressed in TFCs and CpCs in the ovarian niche. (A) Schematic diagram of a gerarium showing the support cell types (namely TFCs, CpCs, and ECs) and the germline cells (including GSCs, cystoblasts [CB], and developing cysts). GSCs are surrounded by 1–2 ECs and they contain an apical organelle called a spectrosome (red), which adopts an elongated shape after GSC asymmetric division. Cystoblasts also

contain spectrosomes, but these are localised randomly within the cell. Cystoblasts undergo four incomplete rounds of division to give rise to 2-, 4-, 8-, and 16-cell cysts interconnected by branched fusomes (red). FCs, follicle cells; FSCs, follicle stem cells. (B) Wild-type (WT) germarium triple stained to visualise the expression of En in TFCs and CpCs (green), α -Spectrin in spectrosomes and fusomes (α -Sp; red), and DNA (blue). (C) Wild-type germarium stained with anti-Hh to visualise TFCs and CpCs (green), anti-Hts to label spectrosomes and fusomes (red), and Hoechst (for DNA; blue). (D) *bab1-Gal4 UAS-nod:GFP* germarium stained with anti-GFP to label TFCs, CpCs, and ECs (albeit with a weaker staining; green) and anti-Hts (red). (E) *ptc-Gal4, UAS-GFP* germarium stained with anti-GFP to label ECs (green), anti-Hts (red), and Hoechst (blue). Asterisks, GSCs; white open arrowheads, wild-type TFCs; yellow open arrowheads, wild-type CpCs; red open arrowheads, wild-type ECs. Scale bars: 10 μ m. doi:10.1371/journal.pbio.1001298.g001

for the wing disc [27,28]. Because the absence of either *hh* or *disp* from other niche cells, such as TFCs or ECs, did not cause a visible GSC phenotype (data not shown), and considering the requirement for Disp in cholesterol-modified-Hh release, these results strongly suggest that Hh needs to be produced in, and secreted from, CpCs to support a stable GSC population.

Activation of the Hh Pathway in ECs Prevents GSC Differentiation

Hh signalling is transduced intracellularly by Hh ligand binding the Patched (Ptc) receptor in receiving cells, allowing the phosphorylation and activation of Smoothed (Smo), a G-protein-coupled receptor normally inhibited by Ptc [29]. In the germarium, Hh ligand produced in the CpCs might act on GSCs

directly, indirectly via ECs, or a combination of the two. To distinguish between these possibilities, we studied the expression pattern of *ptc*, itself a target gene of Hh signalling, as a readout of pathway activation. Analysis of a reporter of *ptc* expression (*ptc-lacZ*) showed expression in ECs but not in CpCs or TFCs (Figure 4A). To corroborate that activation of the *ptc* reporter responded to the canonical Hh pathway, we removed *smo* from ECs to abrogate the Hh response and found that *ptc-lacZ* expression was largely eliminated (100% of cases, $n = 43$; Figure 4B). These results indicate that the Hh pathway is active only in ECs and not in CpCs or TFCs. In fact, the generation of *smo*⁻ CpC clones showed no effect on GSC loss by differentiation (100% of cases, $n = 25$; Figure 4C), whereas the removal of *smo* function from larval/pupal or adult ECs induced GSC differen-

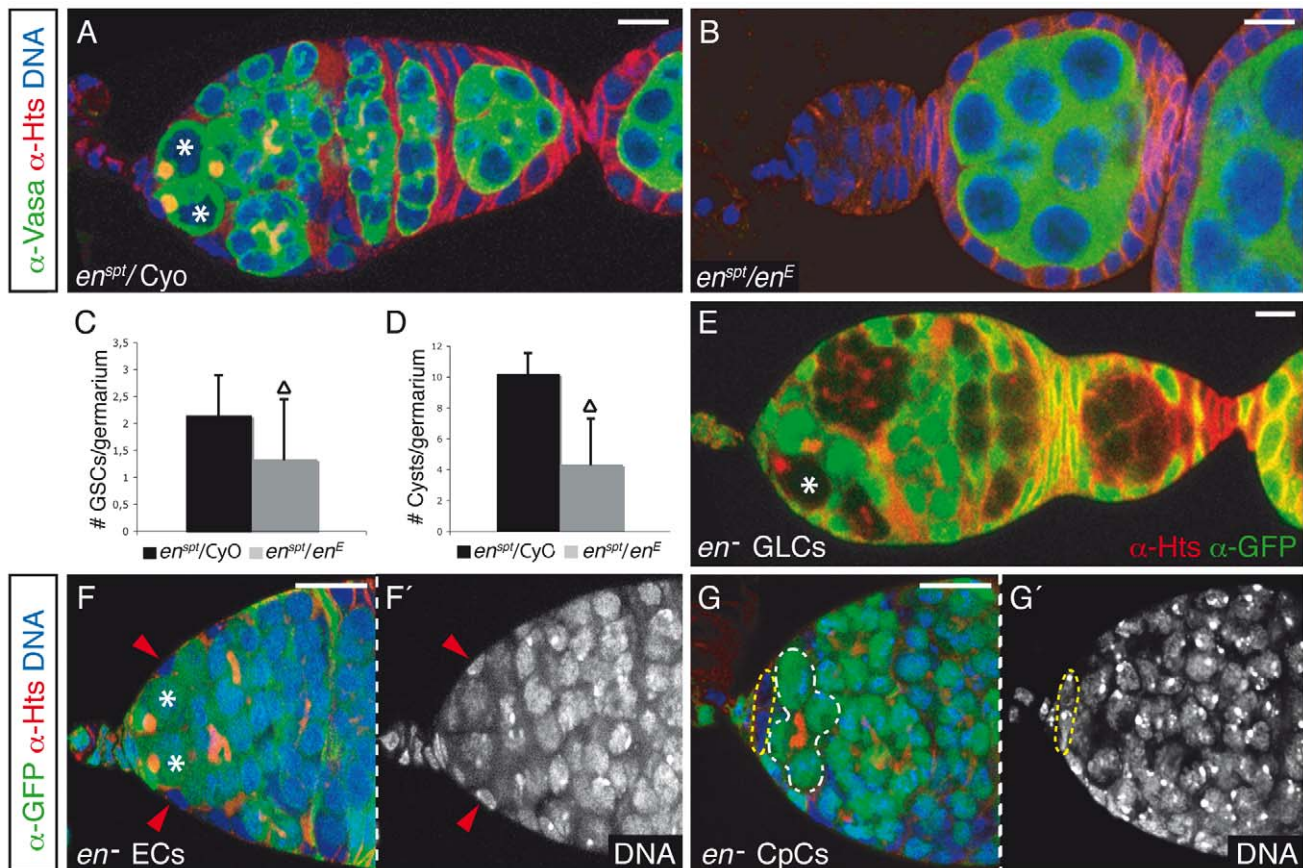


Figure 2. *en* controls germline development. (A and B) Control (A) and experimental (B) germaria dissected after 7 d at restrictive temperature (28°C). While the control germarium shows two GSCs and several differentiating cysts, the mutant is devoid of germline cells. (C and D) Bar chart representations of the mean number of (C) GSCs (\pm standard deviation [s.d.]) and (D) cytotoblasts and developing cysts (\pm s.d.) per germarium in control and experimental germaria. Triangles indicate statistically significant differences (Student's *t* test, $p < 0.0005$). (E) *en^E* germline clones dissected 21 d after heat shock. *en* is not required in the germline. (F) *en^E* EC clones do not affect GSC maintenance. (G) *en^E* CpCs induce GSC differentiation as shown by the appearance of branched fusomes adjacent to the mutant CpCs (see also Figure S2 and Table S1). Somatic clones were induced with the *bab1-Gal4* driver and were dissected 3 d after eclosion. Asterisks, GSCs; GLCs, germline clones; yellow dashed lines, *en* mutant CpCs; white dashed line, four-cell cyst; red arrowheads, *en* mutant ECs. Scale bars: 10 μ m. doi:10.1371/journal.pbio.1001298.g002

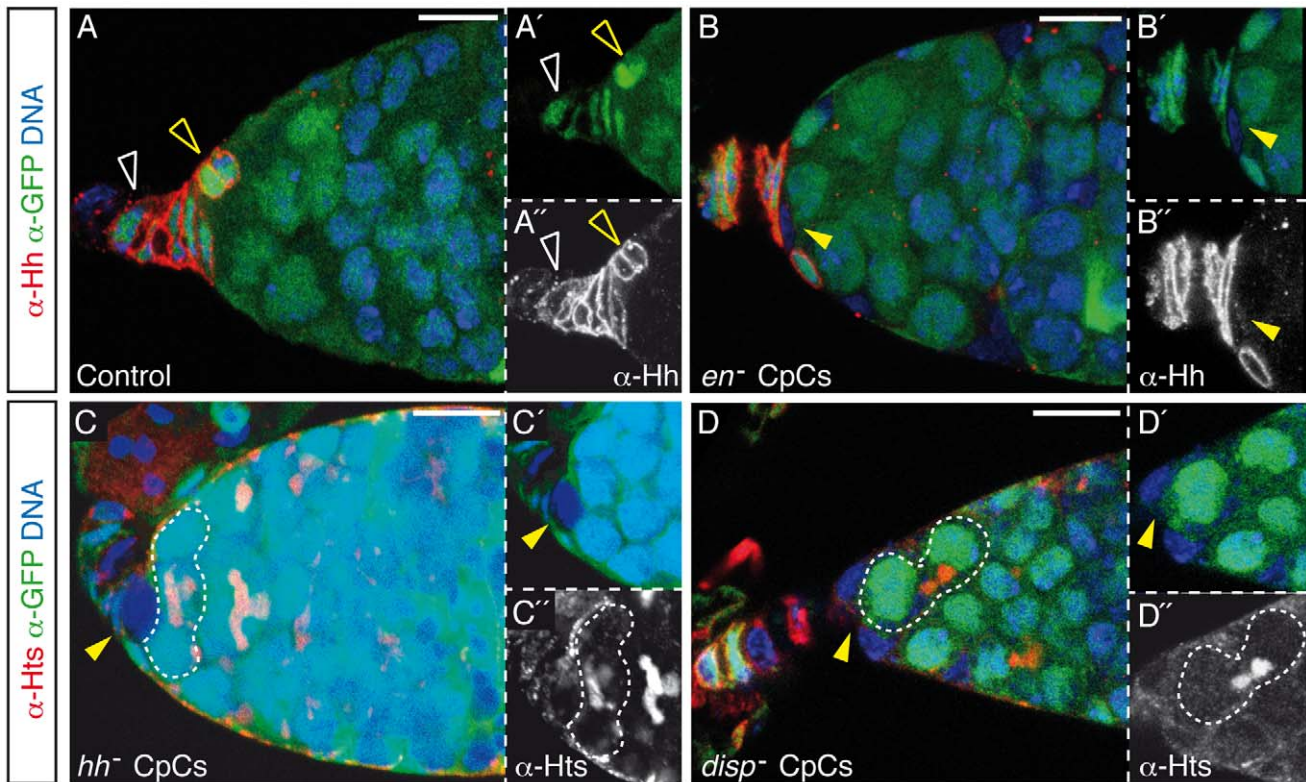


Figure 3. *en* controls Hh protein levels and Hh secretion is required for GSC maintenance. (A) Control germarium. Hh is expressed specifically in TFCs and CpCs. (B) *en^F* mutant CpC showing a strong decrease in Hh levels. (C and D) *hh^{AC}* (C) or *disp^{SH21}* (D) mutant CpCs can induce GSC differentiation, as visualised by the presence of differentiating cysts adjacent to CpCs. See also Figure S3 and Table S2. Ovaries of the appropriate genotypes were dissected 3 d after eclosion. White open arrowheads, wild-type TFCs; yellow open arrowheads, wild-type CpCs; yellow arrowheads, mutant CpCs; white dashed lines, differentiating cysts in contact with CpCs. Scale bars: 10 μ m. doi:10.1371/journal.pbio.1001298.g003

tiation, as visualised by the appearance of branched fusomes within the mosaic niches (69.56% of cases, $n=23$; Figure 4D). Finally, the generation of mutant *sno* germline clones using two different null alleles did not result in any visible phenotypes 7, 14, or 21 d after clone induction (100% of cases, $n>39$ for each genotype and time point; Figure 4E). From these observations, we conclude that Hh produced and secreted by CpCs activates Smo in ECs to elicit a response that is responsible for GSC maintenance.

In an attempt to identify the nature of this response, we measured the mRNA levels of the essential stem cell factors *dpp* and *gbb* in Hh-depleted germaria. Real-time quantitative PCR analysis of *en^{ts}* germaria showed that the levels of *dpp*, *gbb*, and *hh* mRNAs were reduced by more than 60% when compared to control samples (Figure S4). Because *en* is not expressed in ECs, and since *dpp* and *gbb* are transcribed in CpCs and ECs [17,18,22], our data indicate that *en* could regulate *dpp* and *gbb* transcription in ECs via Hh signalling. However, *dpp* has also been shown to be a target of En [30]. To test the possibility that *en* is regulating *dpp* and *gbb* transcription via *hh*, we analysed the amounts of *dpp* and *gbb* mRNAs in ovaries in which the Hh pathway was blocked specifically in ECs for 7 d (*ptc*-Gal4; UAS-*sno* RNAi/*tub*-Gal80^{ts} ovaries). In this experimental condition, the levels of *dpp* and *gbb* mRNAs are diminished by half (Figure 4F). Furthermore, these germaria also show a significant decrease in the number of GSCs per niche (Figure S5; control, 2.7 ± 0.5 GSCs/germarium, $n=40$; experimental, 1.4 ± 0.6

GSCs/germarium, $n=44$). Finally, in order to demonstrate that the expression of *dpp* in ECs is essential for GSC maintenance, we analysed niches in which *dpp* levels were diminished specifically in ECs for 14 d (*ptc*-Gal4; UAS-*dpp* RNAi/*tub*-Gal80^{ts} ovaries). We found a strong reduction in the number of GSCs due to their precocious differentiation (Figures 4G and S5; control, 2.5 ± 0.8 GSCs/germarium, $n=28$; experimental, 1.4 ± 0.6 GSCs/germarium, $n=36$). Considering that these BMP molecules are essential for GSC survival [22,23] and that *dpp* is a target gene of the Hh pathway [31], our results support a model in which female GSC self-renewal requires the *en*-dependent production of Hh in CpCs. Upon secretion by CpCs, Hh juxtacrine signal is transmitted to the adjacent ECs, which in turn control Dpp and Gbb production to sustain GSC maintenance. The fact that the removal of *hh* from CpCs or *sno* from ECs induces a decrease in phospho-Mad levels in the germline, a direct reporter of Dpp signalling, supports this hypothesis (Figure S6). Thus, in addition to the proposed role for CpCs in ovarian niche signalling [32], ECs emerge as important regulators of niche signalling, as they not only are responsible for controlling the Jak/Stat and the EGFR pathways [12,19] but also exert a key role in the regulation of Hh signalling.

CpCs Respond to Impaired Hh Signalling within the Niche by Projecting Hh-Coated Cytosomes

Morphogens exert their effects over long distances, which, in the case of Hh, can be as long as 300 μ m in the vertebrate limb bud

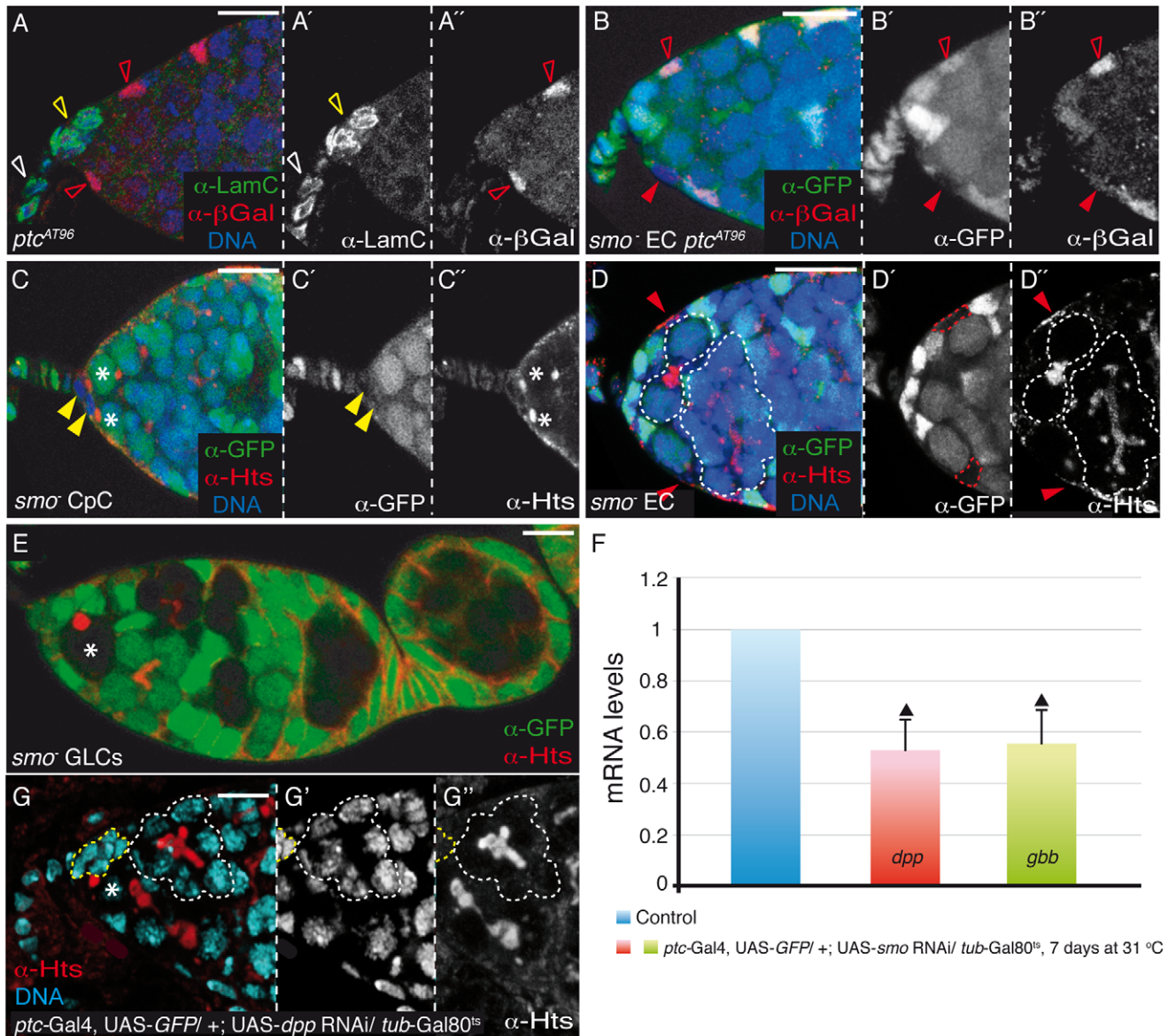


Figure 4. The Hh signalling pathway is required in ECs for GSC maintenance. (A) *ptc*^{AT96} (*ptc-lacZ*) germarium stained to visualise lacZ expression in ECs. Lamin C (LamC) is a marker of TFCs and CpCs. (B) *smo*³ mutant EC showing an undetectable expression of *ptc-lacZ* beyond background levels. (C) *smo*^{D16} mutant CpCs do not induce GSC differentiation. (D) In contrast, *smo*^{D16} mutant ECs are often associated with differentiating cysts. (E) *smo*³ germline clones (GLCs) dissected 21 d after clone induction to show that removal of *smo* from the germ line does not affect GSC development. (F) Real-time quantitative PCR analysis of +; UAS-*smo* RNAi/SM6^ΔTM6B (control) and *ptc-Gal4*, UAS-*GFP*+/+; UAS-*smo* RNAi/*tub-Gal80*^{ts} ovaries kept at 31 °C for 7 d to show that *en* regulates positively *dpp* and *gbb* expression in niche cells. Triangles indicate statistically significant differences (Student's *t* test, *p* < 0.0005). (G) *ptc-Gal4*, UAS-*GFP*+/+; UAS-*dpp* RNAi/*tub-Gal80*^{ts} germarium kept at 31 °C for 14 d displaying a differentiating cyst adjacent to the CpC cluster (see also Figure S5). Somatic clones were induced with the *bab1-Gal4* driver and were dissected 3 d after eclosion. Asterisks, GSCs; white open arrowheads, wild-type TFCs; yellow open arrowheads, wild-type CpCs; red open arrowheads, wild-type ECs; yellow arrowheads, *smo* mutant CpCs; red arrowheads (all panels) and red dashed lines (D'), *smo* mutant ECs; yellow dashed lines, CpC cluster; white dashed lines, differentiating cysts within the niche. Scale bars: 10 μm. doi:10.1371/journal.pbio.1001298.g004

[33]. In contrast, in the *Drosophila* ovarian niche, the Hh-receiving cells adjoin the Hh-producing cells, as ECs directly contact the CpC rosette, which limits the spread of this ligand. To investigate the mechanism by which Hh is transported within the ovarian niche, we analysed in detail the distribution of Hh in the CpCs. The Hh protein is strongly localised to the cell membrane, and in 30.1% of germaria analysed (*n* = 149; Figure 5A), it decorated short cellular projections 0.53 to 1.11 μm in length (0.93 μm on

average) and 0.1 to 0.3 μm in diameter that formed at the CpC–EC boundaries. These narrow, filiform structures were reminiscent of the thin filopodial membranes, called cytonemes, that were initially described in the wing disc. Cytonemes are actin-rich cytoplasmic extensions thought to mediate specific morphogen signalling and to prevent inadequate diffusion of ligands [34–36].

In order to test the biological significance of these structures, we analysed two different experimental scenarios. First, we investi-

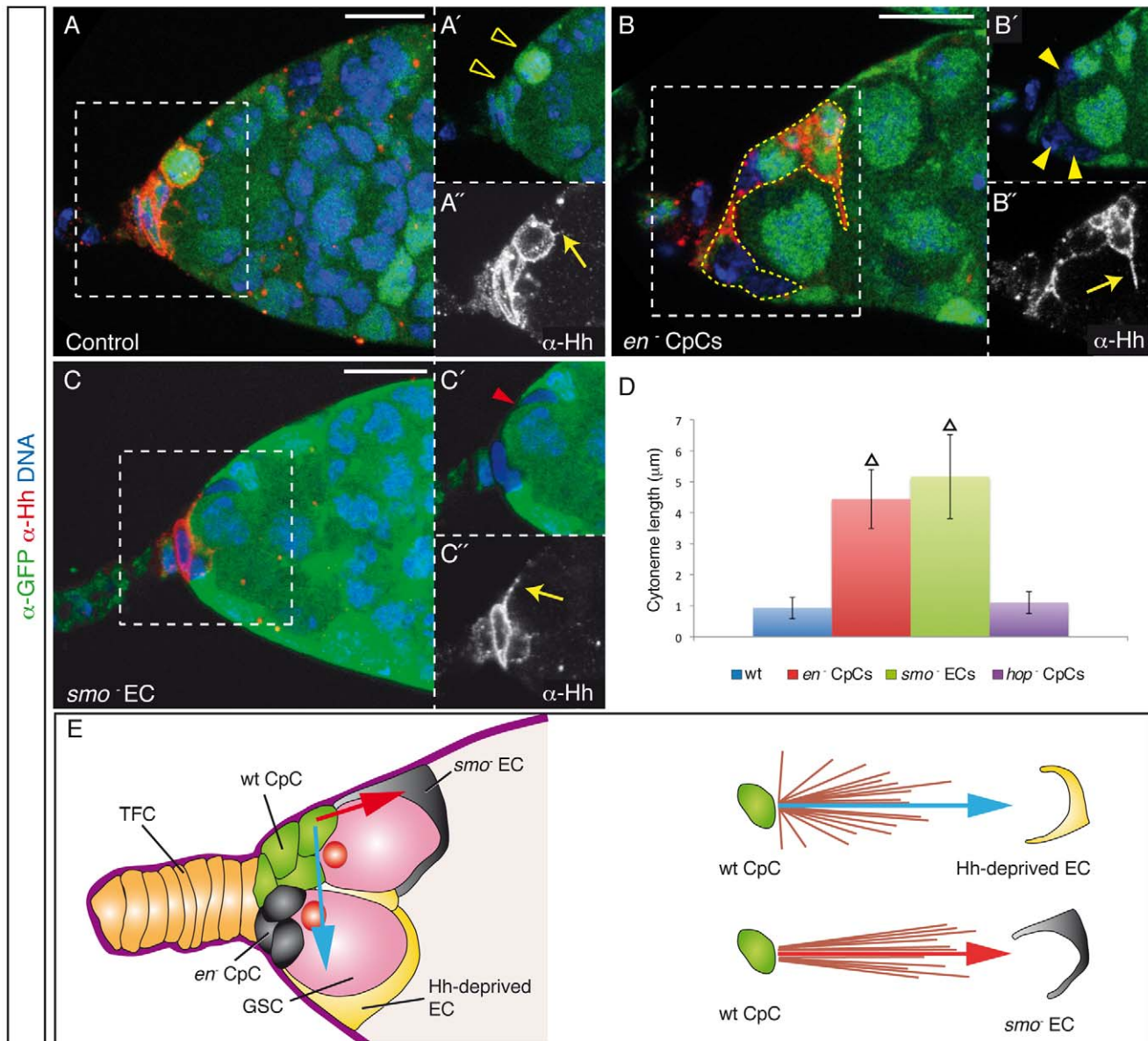


Figure 5. Cytosome-mediated delivery of Hh in the niche. (A) Control germarium showing the typical short cytonemes found in CpCs of wild-type niches. (B) Mosaic germarium containing several *en^E* mutant CpCs and displaying a Hh-coated long cytoneme that originates from a wild-type CpC. (C) A Hh-rich long cytoneme projecting from a wild-type CpC towards a *smo^{D16}* mutant EC. (D) Bar chart representing the mean cytoneme length (\pm s.d.) in control germaria with wild-type (wt) niche cells, and in mosaic germaria containing ≥ 3 *en* mutant CpCs, *smo* mutant ECs, or *hop* mutant CpCs (see also Figure S7 and Tables S3 and S4). Somatic clones were induced with the *bab1-Gal4* driver and were dissected 3 d after eclosion. Triangles indicate statistically significant differences (Student's *t* test, $p < 0.0005$). (E) In order to determine whether the long cytonemes found in the above mosaic germaria projected randomly within the niche, we plotted the position of these cytonemes with respect to two arbitrary axes defined as follows. In each cytoneme-containing germarium, we have drawn a straight arrow that originates in the cytoneme-growing CpC and that is oriented towards either the EC in contact with *en* mutant CpCs ($n = 18$; blue arrow) or the *smo* mutant EC ($n = 11$; red arrow). Our analysis shows that cytonemes grow directionally in the direction of the ECs in contact with *en* mutant CpCs ("Hh-deprived ECs") or towards the *smo* mutant ECs, strongly suggesting that these long filopodia sense, and project to, the signalling-deficient region of the niche. Yellow open arrowheads, wild-type CpCs; yellow arrowheads, *en* mutant CpCs; red arrowhead, *smo* mutant EC; yellow arrows, Hh-coated cytonemes; yellow dashed line, CpC cluster. Scale bars: 10 μ m.

doi:10.1371/journal.pbio.1001298.g005

gated whether these processes would respond to challenging physiological conditions such as deficient Hh niche signalling. To this end, we analysed the distribution of Hh-coated cytonemes in mosaic germaria harbouring *en* mutant CpCs and found that in 54% of these germaria one or two of the remaining wild-type

CpCs displayed thin, Hh-labelled filopodia significantly longer than those of the controls (average size 3.1 μ m, $n = 50$; Figure 5B and 5D). We then blocked the ability of adult ECs to respond to Hh signalling by generating *smo⁻* ECs, and we looked for long cytonemes in these mosaic niches. We found that the absence of

Hh pathway transduction in ECs provoked a response from signalling CpCs in the form of long, Hh-coated cellular extensions detected in 50% of the cases analysed (average size 3.3 μm , $n = 28$; Figure 5C). To discard the possibility that the presence of differentiated cysts within the niche, such as those generated after removing *smo* from ECs, induces long, Hh-positive cytonemes, we generated CpCs mutant for the Jak/Stat kinase *hopscotch*, which also causes GSC differentiation [17,18], and measured cytoneme lengths. In this condition, the cellular processes were not significantly different from those of wild-type controls (average size 1.1 μm , $n = 20$; Figure 5D). Altogether, these results clearly show that the GSC niche can react specifically to decreased Hh levels and/or to impaired Hh signalling by increasing the range of ligand spreading. Moreover, the extended cytonemes found in *en*⁻ or *smo*⁻ mosaic germaria projected towards the signalling-deficient area of the niche (Figure 5E), demonstrating that niche support cells sense, and respond directionally to, spatial signalling cues. Finally, to determine whether these cytonemes are specialised structures developed to mediate niche signalling, we studied the distribution of the adherens junction components DE-Cadherin and Armadillo in cytonemes. These proteins labelled the periphery of wild-type CpCs, delineating their round, regular shape, but were absent from their short cytonemes. Similarly, in mosaic *en*⁻ or *smo*⁻ niches, long cytonemes did not contain DE-Cadherin or Armadillo, which suggests that cytonemes are Hh-coated filopodia grown specifically to deliver a stem cell survival factor rather than a reflection of mere changes in cell shape (Figure S7).

The Hh-Coated Cytonemes Found in Wild-Type CpCs Are Required for GSC Maintenance

Next, we wished to study cytoneme functionality by affecting their formation. Because cytonemes are rich in actin filaments [34], we reasoned that disturbing actin polymerisation in adult CpCs could have an effect specifically on cytoneme production and/or kinetics. Thus, we utilised the *bab1*-Gal4 driver to express modified versions of two known regulators of actin polymerisation in TFCs and CpCs of adult ovaries. We induced the expression of either a constitutively activated form of the *Drosophila* Formin homologue Diaphanus (Dia), Dia^{CA} [37], or a myristoylated form of the Arp2/3-complex regulator Wasp, Wasp^{Myr} [38]. While interfering with actin polymerisation may affect other cellular processes rather than cytoneme formation, we performed several controls to make sure that the observed results were as specific as possible. First, we measured the mean value of fluorescence intensity per area unit in control (*tub*-Gal80^{ts}/+; UAS-*dia*^{CA}/+ or *tub*-Gal80^{ts}/+; UAS-*wasp*^{Myr}/+) or experimental ovaries (*tub*-Gal80^{ts}/+; UAS-*dia*^{CA}/*bab1*-Gal4 or *tub*-Gal80^{ts}/+; UAS-*wasp*^{Myr}/*bab1*-Gal4) kept at 31°C for 5 d upon eclosion to confirm that overexpression of UAS-*wasp*^{Myr} or UAS-*dia*^{CA} in adult germaria affected significantly neither the overall amounts of Hh protein in the niche cells nor the expression of CpC markers such as *bab1* or Lamin C (Figure 6 and data not shown). Second, we manipulated only post-mitotic cells to prevent unwanted effects during mitosis, as we induced ectopic gene expression in adult CpCs. Third, we utilised an experimental setting that did not affect visibly niche morphology or CpC viability. In this scenario, we found that ectopic expression of Wasp^{Myr} or Dia^{CA} for 5 d in niche cells halved the number of germaria growing short cytonemes (from over 30% in controls to 13.6% and 15.4%, respectively, $n > 36$ for each genotype; Figure 6C). Interestingly, this condition also produced a significant decrease in the number of GSCs per niche (from 2.45 \pm 0.7 in controls to 1.8 \pm 0.55 and 1.7 \pm 0.6, respectively, $n > 36$ for each genotype; Figure 6D). Since we did not observe apoptosis above control levels in germline cells

(data not shown) and because we could detect differentiating cysts in these experimental niches (Figure 6B), the formation of short Hh-decorated filopodia in CpCs is an essential step to prevent GSC differentiation. We next tested whether diminishing the number of cytonemes per CpC would affect Hh signalling. To this end, we overexpressed Dia^{CA} in adult TFCs and CpCs utilising the *bab1*-Gal4 driver and monitored the activation of the Hh-signalling reporter *ptc*-lacZ. We found that, in contrast to controls, experimental females grown for 5 d at 31°C largely failed to activate the *ptc*-lacZ reporter in the germarium (Figure 6E and 6F). These results, together with our previous finding that Hh is produced in CpCs and received in ECs, strongly suggest that the Hh-coated cytonemes regulate Hh signalling in the germarium by facilitating Hh delivery to the target ECs to ensure that a normal pool of stem cells is maintained.

Discussion

Niches are dynamic systems often containing stromal cells that provide physical support and survival factors to nurture a population of stem cells. The data presented here demonstrate that the heterotypic association of support cells is crucial for niche function. In the case of the *Drosophila* ovarian niche, it has been previously described that the Jak/Stat pathway regulates the expression of *dpp* in CpCs [17,18]. Our results show that the maintenance of a stable population of GSCs relies also on the coordinated action of the CpCs and the ECs, which allows the production and release of the GSC survival ligand Hh in the CpCs and its reception in the ECs. As a consequence of the transduction of the Hh pathway, ECs produce the stem cell factors Dpp and Gbb (see model in Figure 7). The recent finding of a similar partnership between mesenchymal and haematopoietic stem cells that operates in the bone marrow niche [39] indicates that such collective regulatory interactions within support cells may be a common feature of cellular niches.

The study of the mechanisms behind Hh signalling in the *Drosophila* ovary has allowed the identification of Hh-coated cytonemes in a cellular stem cell niche, emphasising the idea that cytonemes mediate spreading of the activating signal from the producing cells. Recently, it has been reported that the Hh protein localises to long, basal cellular extensions in the wing disk [40]. In addition, filopodial extensions in the wing, eye, and tracheal system of *Drosophila* have been shown to segregate signalling receptors on their surface, thus restricting the activation of signalling pathways in receiving cells [36]. Hence, cytonemes, as conduits for signalling proteins, may be extended by receiving cells—and so are involved in uptake—or may be extended by producing cells—and so are involved in delivery and release.

Interfering with actin polymerisation in adult niches leads to a significant reduction in the number of CpCs growing Hh cytonemes, concomitant with precocious stem cell differentiation, demonstrating that these actin-rich structures are required to prevent stem cell loss and thus are functionally relevant. Importantly, because we disturbed actin dynamics in post-mitotic CpCs that still produce wild-type levels of Hh protein and express CpC markers (but fail to activate the Hh pathway in ECs), the observed effects on stem cell maintenance are most likely specific to Hh delivery from CpCs to their target ECs via short cytonemes. This interpretation is further reinforced by the observation that CpCs can sense decreased Hh levels and/or a dysfunction in the transduction of the Hh pathway in the niche and respond to it by growing Hh-rich membrane bridges up to 6-fold longer than in

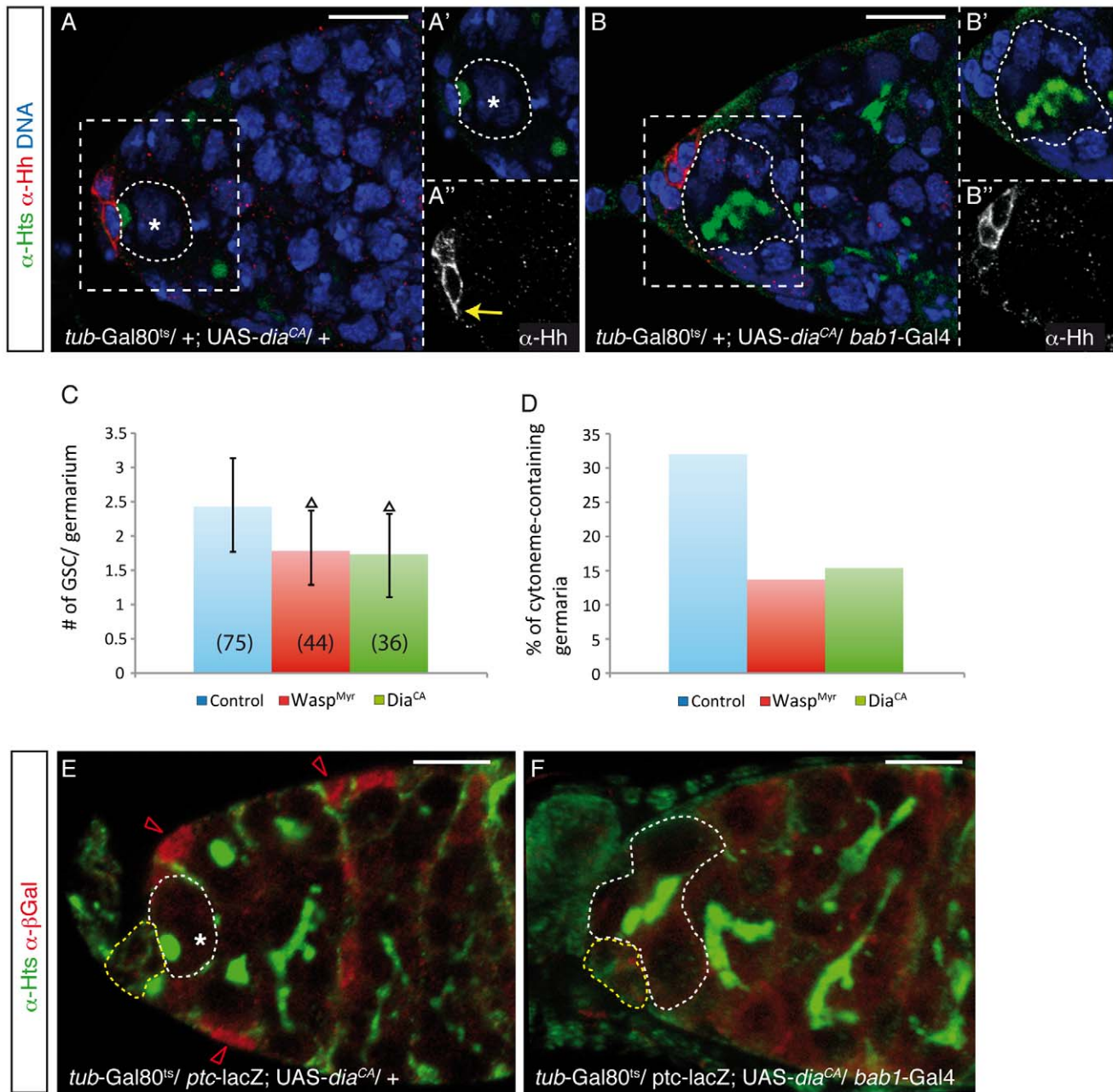


Figure 6. Hh-decorated cytonemes are required for GSC maintenance. (A and F) Germaria from females grown at 18°C and transferred to 31°C for 5 d upon eclosion. (A and B) Ovaries stained with anti-Hh (red) to mark cytonemes and anti-Hts (green) to label the spectrosomes and fusomes of germline cells. (A) Control germarium from a *tub-Gal80^{ts/+}; UAS-dia^{CA}/+* female displaying a short cytoneme (yellow arrow). (B) Experimental germarium from a *tub-Gal80^{ts/+}; bab1-Gal4/UAS-dia^{CA}* female. In this condition, the percentage of germaria showing short cytonemes and the number of GSCs per germarium are significantly lower than in controls. (C and D) Bar charts representing the mean number of GSCs (\pm s.d.) per germarium (C) or the percentage of germaria showing short cytonemes (D) in control *tub-Gal80^{ts/+}; UAS-wasp^{Myr}* (or *UAS-dia^{CA}/+*) and in experimental *tub-Gal80^{ts/+}; bab1-Gal4/UAS-wasp^{Myr}* (*Wasp^{Myr}*) and *tub-Gal80^{ts/+}; bab1-Gal4/UAS-dia^{CA}* (*Dia^{CA}*) germaria. The number of germaria analysed for each experiment (*n*) is shown. Black triangles indicate a statistically significant difference between the given experimental condition and the control (Student's *t* test, $p < 0.01$). The percentages of experimental germaria containing cytonemes were significantly different from controls with a probability of 95% (Chi-square test). (E and F) The overexpression of *Dia^{CA}* largely abrogates the activation of the Hh pathway in ECs, as shown by the absence of *ptc-lacZ* expression—a target of the pathway—in experimental germaria. Asterisks, GSCs; red open arrowheads, ECs showing *ptc-lacZ* expression; yellow dashed lines, CpC clusters; white dashed lines, GSCs in (A) and (E) and differentiating cysts within the niche in (B) and (F). Scale bars: 10 μ m.

doi:10.1371/journal.pbio.1001298.g006

controls. In this regard, it is interesting to note that the two lipid modifications found in mature Hh act as membrane anchors and give secreted Hh a high affinity for membranes and signalling

capacities [41,42]. In fact, it has been recently described that a lipid-unmodified form of Hh unable to signal does not decorate filopodia-like structures in the wing imaginal disc epithelium,

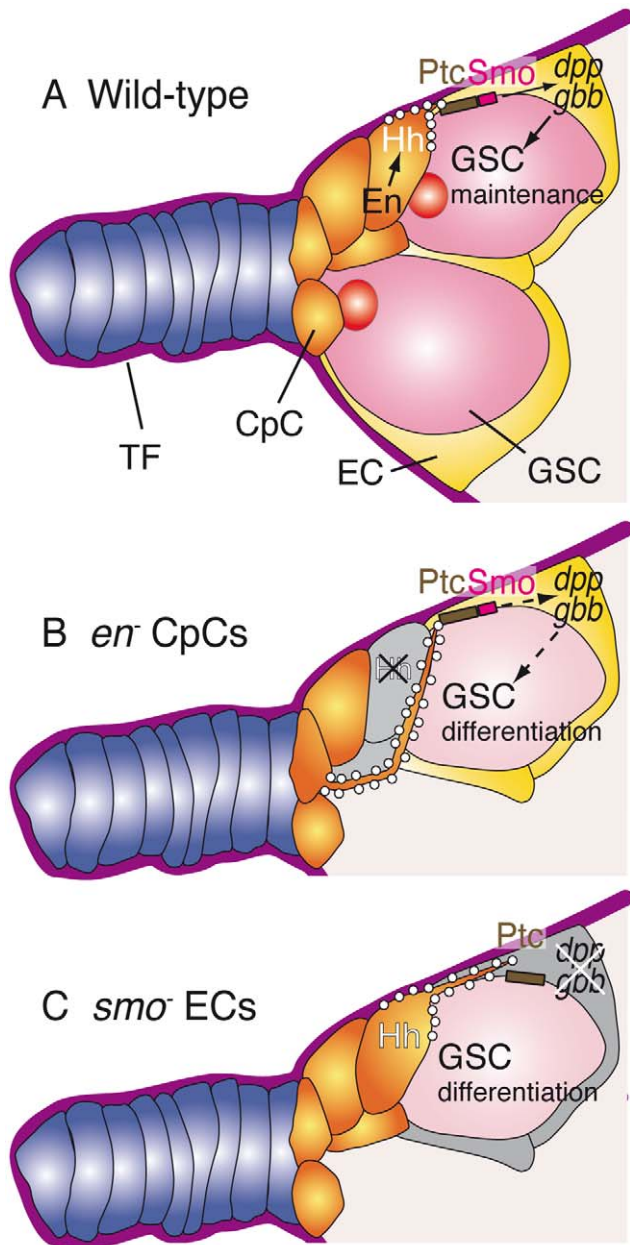


Figure 7. A model for the response of the GSC niche to low levels of Hh signalling. (A) In wild-type niches En regulates Hh production in CpCs, which is then delivered to the neighbouring ECs via short, thin cytoplasmic extensions. Upon binding to the Ptc receptor, thus releasing Smo from inhibition, the Hh signal is transduced in ECs to regulate Dpp and Gbb production, which in turn act as survival factors to maintain the GSC population within the niche. (B) Mosaic niche containing *en* mutant CpCs unable to produce the Hh ligand. As a result, the transcription of the *dpp* and *gbb* genes in the adjacent ECs is compromised, resulting in GSC loss. Wild-type CpCs respond to this deficiency in Hh levels by directing Hh-rich long cytonemes towards the Hh-deprived ECs. (C) Blocking *smo* function prevents target gene activation and causes GSC depletion. Wild-type CpCs react to this deficient readout of Hh signalling by projecting Hh-coated long cytonemes towards the *smo* mutant ECs. doi:10.1371/journal.pbio.1001298.g007

confirming the link between Hh transport along cytonemes and Hh signalling [40]. Thus, cytonemes may ensure specific targeting of the Hh ligand to the receiving germline cells in a context of

intense signalling between niche cells and the GSCs. Interestingly, in both *en*⁻ and *smo*⁻ mosaic niches, the long processes projected towards the signalling-deficient area of the niche, which showed that competent CpCs sense the strength of Hh signalling activity in the microenvironment. While the nature of the signal perceived by the CpCs or the receptor(s) involved in the process are unknown, we postulate that Hh-decorated filopodial extensions represent the cellular synapsis required for signal transmission that is established between the Hh-producing cells (the CpCs) and the Hh-receiving cells (the ECs). In this scenario—and because Ptc, the Hh receptor, is a target of the pathway—the membranes of mutant ECs, in which the transduction of the pathway is compromised, contain lower Ptc levels. Thus, longer and perhaps more stable projections ought to be produced to allow proper signalling. In addition, the larger the number of *en* mutant cells (and hence the stronger the deficit in Hh ligand concentration or target gene regulation), the longer the cellular projections decorated with Hh (Tables S3 and S4), which indicates that the niche response is graded depending on the degree of signalling shortage.

Do the longer cytonemes found in mosaic germaria represent structures created de novo, or do they simply reflect a pre-existing meshwork of thin intercellular bridges that can regulate the amount of Hh protein in transit across them? Because we utilised an anti-Hh antibody to detect the cytonemes and all of our attempts to identify other markers for these structures have failed, we cannot presently discriminate between these two possibilities. In any case, since we did not detect increased Hh levels in wild-type CpCs that contained cytonemes relative to those that did not, it is clear that long filopodia do not arise solely by augmenting Hh production in the CpCs. Rather, if long cytonemes are not synthesised in response to a Hh signalling shortage and if they already existed in the niche, they ought to restrict Hh spreading independently of significant Hh production. Furthermore, because the strength of Hh signalling in the niche determines the distance of Hh spreading, either cytoneme growth or Hh transport (or both) are regulated by the ability of the CpCs to sense the Hh signalling output.

Our demonstration that a challenged GSC niche can respond to insufficient signalling by the cytoneme-mediated delivery of the stem cell survival factor Hh over long distances has wider implications. Niche cells have been shown to send cellular processes to their supporting stem cells in several other scenarios: the *Drosophila* ECs of the ovary and the lymph gland, the ovarian niche of earwigs, and the germline mitotic region in the hermaphrodite *Caenorhabditis elegans* [5,6,14,43,44]. Similarly, wing and eye disc cells project cytonemes to the signalling centre of the disc [34,36]. However, definitive proof that the thin filopodia described in the lymph gland, the earwig ovary, or imaginal discs deliver signals from the producing to the effector cells is lacking. Our findings strongly suggest that cytonemes have a role in transmitting niche signals over distance, a feature that may underlie the characteristic response of more complex stem cell niches to challenging physiological conditions. Careful analysis of the architecture of sophisticated niches, such as the bone marrow trabecular zone for mouse haematopoietic stem cells, will be needed to further test this hypothesis and to determine whether it represents a conserved mechanism for stem cell niche signalling.

Materials and Methods

Fly Stocks

Flies were grown at 25°C on standard medium for *Drosophila*. The following genetically null alleles were used: *en*^E, *en*⁵⁴ [45], *hh*²¹,

hh^{AC} [46], *disp^{SH21}* [28], *smo^{D16}* [47], and *smo³* [48]. *ptc^{AT96}* is a *LacZ* enhancer trap inserted in the gene [49]. *en^{SP1}* [50] is a temperature-sensitive allele. To express UAS-*DsRed* and UAS-*flp* we used the *bab1-Gal4* line [51]. The expression of UAS transgenes in ECs was done utilising the *ptc-Gal4* driver. In order to generate experimental *en^{SP1/en^E}* adult females, flies were shifted from 25°C to 28°C for 7 or 14 d upon eclosion.

To obtain adult females overexpressing Wasp^{Myr} [38] or Dia^{CA} [37], *w; tub-Gal80^{IS}/CyO; bab1-Gal4/TM2* flies were crossed to *w; UAS-wasp^{Myr}* or *w; UAS-dia^{CA}*, respectively. To overexpress *dpp* RNAi (VDRIC) or *smo* RNAi (Bloomington Stock Center) in ECs, *w; ptc-Gal4, UAS-GFP; tub-Gal80^{IS}/SM6^ΔTM6B* flies were crossed to *w; UAS-dpp* RNAi, *w; UAS-smo* RNAi. The offspring were grown at 18°C, and upon eclosion adult F1 flies were shifted to 31°C for 5, 7, or 14 d.

Immunohistochemistry and Image Analysis

Ovaries were dissected at room temperature in PBS containing 0.1% Tween-20 (PBT), fixed for 20 min with 4% PFA, blocked with PBT+10% BSA for 1 h, and washed in PBT before they were incubated for 15 h with primary antibodies diluted in PBT supplemented with 1% BSA. Primary antibodies were washed three times in PBT containing 1% BSA. Secondary antibodies were diluted in PBT containing 0.1% BSA. Primary antibodies were used at the following concentrations: mouse anti-Hts (1B1) (Developmental Studies Hybridoma Bank [DSHB], University of Iowa), 1:50; rabbit anti-Vasa (a gift from R. Lehmann), 1:1,000; mouse anti-En (4D9) (DSHB), 1:50; rabbit anti- α -Spectrin (a gift from R. Dubreuil), 1:400; rabbit anti-GFP (Molecular Probes), 1:500; mouse anti-GFP (Molecular Probes), 1:50; mouse anti-Lamin C (LC28.26) (DSHB), 1:50; rabbit anti-Hh (a gift from S. Eaton [52]), 1:500; rabbit anti-phospho-Mad 1/5/8 (a gift from E. Laufer), 1:5,000; rabbit anti- β -galactosidase (Cappel), 1:1,000; rabbit anti-cleaved Caspase 3 (BioLabs), 1:50; and mouse anti-Orb (6H4+4H8) (DSHB), 1:50. Secondary antibodies (Cy2- and Cy3-conjugated, Jackson ImmunoResearch) were used at 1:100. DNA staining was performed using the DNA dye Hoechst (Sigma) at 1:1,000. Images were captured with a Leica SPE confocal microscope and processed using ImageJ, Adobe Photoshop, and Adobe Illustrator.

Fluorescence intensity units and cytoneme length were measured using the Leica LAS-AF software. Images were captured with a Leica SPE confocal microscope and processed using ImageJ, Adobe Photoshop, and Adobe Illustrator.

Generation of Somatic and Germline Mitotic Clones

To generate mitotic clones we induced the Flipase enzyme using either a heat shock promoter or the *bab1-Gal4* driver to activate expression of a UAS-*flp* construct. *en* and *smo* mutant germline clones were induced by giving 3-d-old females two 1-h-long heat shocks at 37°C spaced by 10 h at 25°C. *hh*, *disp*, *en*, and *smo* mutant somatic clones were induced expressing UAS-*flp* with the *bab1-Gal4* driver. Ovaries were processed 3 d (for somatic clones) or 7, 14, or 21 d (for germline clones) after treatment. To eliminate *smo* function in adult females, 3-d-old HS-*flp¹¹¹²/+*; *smo^{D16}* FRT40A/*ubi-nls:GFP* FRT40A flies were subjected to three 1-h-long heat shocks at 37°C separated by 6-h periods at 25°C. The following chromosomes were used: HS-*flp¹¹¹²*, FRT42D *en⁵⁴*, FRT42D *en^E*, FRT42D *ubi-nls:GFP*, *smo^{D16}* FRT40A, *ubi-nls:GFP* FRT40A, FRT42D *ubi-nls:GFP*, *hh^{AC}* FRT82B, *hh²¹* FRT82B, *disp^{SH21}* FRT82B, *bab1-Gal4* FRT82B *ubi-nls:GFP*, UAS-*flp*, *smo³* FRT40A *ptc^{AT96}*, and *bab1-Gal4* UAS-*flp*.

Quantification of *hh*, *dpp*, and *gbb* mRNA Levels

The relative amounts of *hh*, *dpp*, and *gbb* mRNAs were determined by real-time quantitative PCR using the comparative cycle threshold (*C_T*) method [53], Fam-dye-labelled TaqMan MGB probes (Applied Biosystems), and an ABI-PRISM 7700 Sequence Detection System. RNA polymerase II (*RpIII40*) was used to normalise mRNA levels. *hh*, *dpp*, or *gbb* mRNA relative amount was calculated from the determination of the difference between the *C_T* of the given gene and that of *RpIII40*. *C_T* values used were the result of three different replicas from three independent experiments. Primers and TaqMan probes for the different cDNAs were obtained from the Assays-by-Design Service (Applied Biosystems) with the following sequences (5′–3′): *RpIII40*, forward, ACTGAAATCATGATGTACGACAACGA, reverse, TGAGAGATCTCCTCGGCATTCT, probe, TCCTC-GTACAGTTCTTCC; *hh*, forward, GCAGGCGCCACATC-TACT, reverse, GCACGTGGGAAGTATGATCGA, probe, CCG-TCAAGTCAGATTTCG; *dpp*, forward, GCCAACACAGTGCG-AAGTTTTTA, reverse, TGGTGCGGAAATCGATCGT, probe, CACACAAAGATAGTAAAATC; *gbb*, forward, CGCTGTCC-TCGGTGAACA, reverse, CGGTCACGTTGAGCTCCAA, probe, CCAGCCCACGTAGTCC.

cDNA was synthesised from ~100–200 ovary pairs of the following characteristics: *en^{SP1}/CyO* (control) and *en^{SP1/en^E}* (experimental) females were shifted from 25°C to 28°C for 7 d after eclosion prior to dissection. +; UAS-*smo* RNAi/SM6^ΔTM6B (control) and *ptc-Gal4, UAS-GFP/+; UAS-smo* RNAi/*tub-Gal80^{IS}* (experimental) females were shifted from 25°C to 31°C for 7 d after eclosion prior to dissection.

Statistical Analysis

A Student's *t* test was used to determine whether the following were significantly different between control and experimental samples: (i) the mean number of GSCs and differentiated cysts per germarium, (ii) the relative levels of *hh*, *dpp*, and *gbb* expression, and (iii) the length of cytonemes. To analyse whether the observed differences in the percentages of cytoneme-containing germaria between control ovaries and ovaries overexpressing Wasp^{Myr} or Dia^{CA} were significant, we applied the Chi-square test. Differences were considered significant when the *p*-values were less than 0.01.

Supporting Information

Figure S1 Loss of *en* function in CpCs induces GSC differentiation. This supplemental figure is related to Figure 2. (A–C) FRT42D *en^E/FRT42D ubi-nls:GFP; bab1-Gal4* UAS-*flp* germaria. (A and A') Control germarium stained with anti-Orb (red), anti-GFP (green), and Hoechst (white) to show the progressive accumulation of Orb protein in the oocyte of differentiating cysts. (B and B') Experimental germarium containing *en* mutant CpCs. The germline cyst adjacent to the CpCs already shows Orb protein accumulated in a single cell, a characteristic of mature 16-cell cysts. (C and C') Germarium stained with the apoptotic marker anti-Caspase 3 to show that the loss of *en* in the CpCs does not induce GSC apoptosis. Rather, these cells enter differentiation. Asterisks, GSCs; yellow open arrowheads, wild-type CpCs; yellow dashed lines, *en* mutant CpCs; white dashed lines, differentiating germline cysts. Scale bars: 10 μ m. (PDF)

Figure S2 The loss of *en* does not affect CpC fate. This supplemental figure is related to Figure 2. (A–A'') FRT42D *en^E/FRT42D ubi-nls:GFP; bab1-Gal4* UAS-*flp* germarium stained with anti-Lamin C to visualise TFCs and CpCs (red), anti-GFP to mark

mutant cells (green), and Hoechst (for DNA; blue). (B–B') *w*; UAS-*DsRed*; FRT42D *en^E*/FRT42D *ubi-nls*:GFP; *bab1*-Gal4 UAS-*flp* germarium stained with anti-GFP to mark mutant cells (green) and Hoechst (for DNA; blue). The autofluorescence of the DsRed protein was observed directly. The expression of the *bab1* gene and of Lamin C protein are not altered in *en* mutant CpCs (yellow arrowheads). Scale bars: 10 μ m. (PDF)

Figure S3 Hh-positive cells at the base of the terminal filament express the CpC marker Lamin C. This supplemental figure is related to Figure 3. (A–A') Wild-type germarium stained with anti-Lamin C (red), anti-Hh (green), and Hoechst (blue). Yellow open arrowheads, wild-type CpCs. Scale bar: 10 μ m. (PDF)

Figure S4 *hh*, *dpp*, and *gbb* mRNA levels are decreased in *en^{SPt}* mutant ovaries. This supplemental figure is related to Figure 4. Real-time quantitative PCR analysis of *en^{SPt}*/CyO (control) and *en^{SPt}*/*en^E* ovaries kept at 28°C for 7 d to show that *en* regulates positively *hh*, *dpp*, and *gbb* expression in niche cells. In wild-type germaria, *en* is expressed in TFCs and CpCs. Triangles indicate statistically significant differences (Student's *t* test, $p < 0.0005$). (PDF)

Figure S5 The reduction of *dpp* or *smo* mRNA levels in ECs induces GSC loss. This supplemental figure is related to Figure 4. Overexpression of *dpp* or *smo* RNAi in ECs utilising the *ptc*-Gal4 driver reduces the number of GSCs per germarium. Control females (+; UAS-*dpp* RNAi/SM6^ΔTM6B and +; UAS-*smo* RNAi/SM6^ΔTM6B) and experimental females (*ptc*-Gal4, UAS-*GFP*/+; UAS-*dpp* RNAi/*tub*-Gal80^{ts} or *ptc*-Gal4, UAS-*GFP*/+; UAS-*smo* RNAi/*tub*-Gal80^{ts}) were transferred from 18°C to 31°C for 7 or 14 d after eclosion. The total amount of GSCs per germarium was determined by counting the number of spectroscopy-containing germline cells in contact with CpCs. Triangles indicate statistically significant differences (Student's *t* test, $p < 0.0001$). The sample size (number of germaria analysed) is shown for each genotypic class. (PDF)

Figure S6 The activity of the *dpp* pathway in the germline depends on the expression of *hh* in CpCs or that of *smo* in ECs. This supplemental figure is related to Figure 4. (A and B) UAS-*flp*/+; FRT82B *hh^{AC}*/*bab1*-Gal4 FRT82B *ubi-nls*:GFP and (C) *smo^{D16}* FRT40A/*ubi-nls*:GFP FRT40A; *bab1*-Gal4 UAS-*flp*/+ germaria stained with anti-phospho-Mad (red), anti-GFP (green), and Hoechst (blue) to show that the activation of the *dpp* pathway—and thus the expression of phospho-Mad—in the GSCs and cystoblasts depends on the production of Hh in the CpCs and the activation of its pathway via Smo in the ECs. (A and A') Control germarium showing the accumulation of phospho-Mad in GSCs (white asterisks) and, to a lesser extent, in cystoblasts (yellow asterisks). (B and C) Experimental germaria containing *hh* mutant CpCs (B and B') or *smo* mutant ECs (C and C'). Germline cells adjacent to mutant cells do not express detectable levels of phospho-Mad. White asterisks, GSCs; yellow asterisk, cystoblast; yellow open arrowheads, wild-type CpCs; red open arrowheads, wild-type ECs;

yellow arrowheads, *hh* mutant CpCs; red arrowheads, *smo* mutant ECs. Scale bars: 10 μ m. (PDF)

Figure S7 Projected cytonemes do not contain the adherent junction components Armadillo or DE-Cadherin. This supplemental figure is related to Figure 5. (A) In wild-type niches, Hh and Armadillo co-localise at the cell periphery in CpCs. (B and C) FRT42D *en^E*/FRT42D *ubi-nls*:GFP; *bab1*-Gal4 UAS-*flp* mosaic germaria containing *en* mutant cells and stained for anti-Hh and anti-Arm (B) or anti-DE-Cadherin (C). In these mosaic germaria, some wild-type CpCs project long cytonemes decorated with Hh protein. However, these filopodia do not contain DE-Cadherin or Armadillo. Yellow open arrowheads point to CpCs. Yellow arrows demarcate Hh-containing cytonemes. Yellow open arrows indicate the absence of DE-Cadherin or Armadillo in these filopodia. Scale bars: 10 μ m. (PDF)

Table S1 The number of GSCs per germarium depends on *en* activity. This supplemental table is related to Figure 1. The percentage of germaria containing 0, 1, or 2–3 GSCs is shown for four different genotypes. Females were shifted from 25°C to 28°C for 7 d upon eclosion and prior to dissection. (DOC)

Table S2 The average number of GSCs in mosaic germaria depends on the number of *hh* mutant CpCs. This supplemental table is related to Figure 5. The table shows the average number of GSCs in control and experimental germaria containing ≤ 2 or ≥ 3 *hh* mutant CpCs. (DOC)

Table S3 Average cytoneme length in different experimental conditions. This supplemental table is related to Figure 5. The table shows the average length (in micrometers) of cytonemes that project from wild-type CpCs in wild-type controls and in mosaic germaria containing 1, ≤ 2 , or ≥ 3 mutant cells. (DOC)

Table S4 Total cytoneme length per CpC in different experimental conditions. This supplemental table is related to Figure 5. The table shows the average length (in micrometers) of all cytonemes per CpC in wild-type controls and in mosaic germaria containing 1, ≤ 2 , or ≥ 3 mutant cells. (DOC)

Acknowledgments

We thank A. Casali, F. Casares, S. Eaton, E. Laufer, the Developmental Studies Hybridoma Bank (University of Iowa), the VDRC, and the Bloomington Stock Center for fly stocks and reagents; J. Culi, B. Estrada, M. D. Martín-Bermudo, J. R. Pearson, and A. E. Rosales-Nieves for comments on the manuscript; and R. Faleiro (I. Guerrero's laboratory) for sharing before publication her results on the role of Wasp^{Myr} and Dia^{CA} in cytoneme formation in the wing disc.

Author Contributions

The author(s) have made the following declarations about their contributions: Conceived and designed the experiments: PR-R IG AG-R. Performed the experiments: PR-R AG-R. Analyzed the data: PR-R AG-R. Contributed reagents/materials/analysis tools: PR-R IG AG-R. Wrote the paper: PR-R IG AG-R.

References

- Morrison SJ, Spradling AC (2008) Stem cells and niches: mechanisms that promote stem cell maintenance throughout life. *Cell* 132: 598–611.
- Scadden DT (2006) The stem-cell niche as an entity of action. *Nature* 441: 1075–1079.

3. Traiffort E, Angot E, Ruat M (2010) Sonic Hedgehog signaling in the mammalian brain. *J Neurochem* 113: 576–590.
4. Brabletz S, Schmalhofer O, Brabletz T (2009) Gastrointestinal stem cells in development and cancer. *J Pathol* 217: 307–317.
5. Mandal L, Martinez-Agosto JA, Evans CJ, Hartenstein V, Banerjee U (2007) A Hedgehog- and Antennapedia-dependent niche maintains *Drosophila* haematopoietic precursors. *Nature* 446: 320–324.
6. Krzemien J, Dubois L, Makki R, Meister M, Vincent A, et al. (2007) Control of blood cell homeostasis in *Drosophila* larvae by the posterior signalling centre. *Nature* 446: 325–328.
7. Takashima S, Mkrtchyan M, Younossi-Hartenstein A, Merriam JR, Hartenstein V (2008) The behaviour of *Drosophila* adult hindgut stem cells is controlled by Wnt and Hh signalling. *Nature* 454: 651–655.
8. McMahon AP, Ingham PW, Tabin CJ (2003) Developmental roles and clinical significance of hedgehog signaling. *Curr Top Dev Biol* 53: 1–114.
9. Varjosalo M, Taipale J (2008) Hedgehog: functions and mechanisms. *Genes Dev* 22: 2454–2472.
10. Pearson J, Lopez-Onieva L, Rojas-Rios P, Gonzalez-Reyes A (2009) Recent advances in *Drosophila* stem cell biology. *Int J Dev Biol* 53: 1329–1339.
11. Song X, Zhu C-H, Doan C, Xie T (2002) Germline stem cells anchored by adherens junctions in the *Drosophila* ovary niches. *Science* 296: 1855–1857.
12. Decotto E, Spradling AC (2005) The *Drosophila* ovarian and testis stem cell niches: similar somatic stem cells and signals. *Dev Cell* 9: 501–510.
13. Kirilly D, Xie T (2007) The *Drosophila* ovary: an active stem cell community. *Cell Res* 17: 15–25.
14. Kirilly D, Wang S, Xie T (2011) Self-maintained escort cells form a germline stem cell differentiation niche. *Development* 138: 5087–5097.
15. Morris LX, Spradling AC (2011) Long-term live imaging provides new insight into stem cell regulation and germline-soma coordination in the *Drosophila* ovary. *Development* 138: 2207–2215.
16. Ward EJ, Shcherbata HR, Reynolds SH, Fischer KA, Hatfield SD, et al. (2006) Stem cells signal to the niche through the Notch pathway in the *Drosophila* ovary. *Curr Biol* 16: 2352–2358.
17. Lopez-Onieva L, Fernandez-Minan A, Gonzalez-Reyes A (2008) Jak/Stat signalling in niche support cells regulates dpp transcription to control germline stem cell maintenance in the *Drosophila* ovary. *Development* 135: 533–540.
18. Wang L, Li Z, Cai Y (2008) The JAK/STAT pathway positively regulates DPP signaling in the *Drosophila* germline stem cell niche. *J Cell Biol* 180: 721–728.
19. Liu M, Lim TM, Cai Y (2010) The *Drosophila* female germline stem cell lineage acts to spatially restrict DPP function within the niche. *Sci Signal* 3: ra57.
20. Doctor JS, Jackson PD, Rashka KE, Visalli M, Hoffmann FM (1992) Sequence, biochemical characterization, and developmental expression of a new member of the TGF-beta superfamily in *Drosophila melanogaster*. *Dev Biol* 151: 491–505.
21. Wharton KA, Thomsen GH, Gelbart WM (1991) *Drosophila* 60A gene, another transforming growth factor beta family member, is closely related to human bone morphogenetic proteins. *Proc Natl Acad Sci U S A* 88: 9214–9218.
22. Song X, Wong MD, Kawase E, Xi R, Ding BC, et al. (2004) Bmp signals from niche cells directly repress transcription of a differentiation-promoting gene, bag of marbles, in germline stem cells in the *Drosophila* ovary. *Development* 131: 1353–1364.
23. Xie T, Spradling A (1998) decapentaplegic is essential for the maintenance and division of germline stem cells in the *Drosophila* ovary. *Cell* 94: 251–260.
24. Forbes A, Lin H, Ingham P, Spradling A (1996) hedgehog is required for the proliferation and specification of ovarian somatic follicle cells prior to egg chamber formation in *Drosophila*. *Development* 122: 1125–1135.
25. Jiang J, Hui CC (2008) Hedgehog signaling in development and cancer. *Dev Cell* 15: 801–812.
26. King F, Szakmary A, Cox D, Lin H (2001) Yb modulates the divisions of both germline and somatic stem cells through piwi- and hh-mediated mechanisms in the *Drosophila* ovary. *Mol Cell* 7: 497–508.
27. Burke R, Nellen D, Bellotto M, Hafén E, Senti KA, et al. (1999) Dispatched, a novel sterol-sensing domain protein dedicated to the release of cholesterol-modified hedgehog from signaling cells. *Cell* 99: 803–815.
28. Amanai K, Jiang J (2001) Distinct roles of Central missing and Dispatched in sending the Hedgehog signal. *Development* 128: 5119–5127.
29. Hooper JE, Scott MP (2005) Communicating with Hedgehogs. *Nat Rev Mol Cell Biol* 6: 306–317.
30. Dahmann C, Basler K (2000) Opposing transcriptional outputs of Hedgehog signaling and engrailed control compartmental cell sorting at the *Drosophila* A/P boundary. *Cell* 100: 411–422.
31. Torroja C, Gorfinkel N, Guerrero I (2005) Mechanisms of Hedgehog gradient formation and interpretation. *J Neurobiol* 64: 334–356.
32. Song X, Call GB, Kirilly D, Xie T (2007) Notch signaling controls germline stem cell niche formation in the *Drosophila* ovary. *Development* 134: 1071–1080.
33. Zhu AJ, Scott MP (2004) Incredible journey: how do developmental signals travel through tissue? *Genes Dev* 18: 2985–2997.
34. Ramirez-Weber F-A, Kornberg T (1999) Cytosomes: cellular processes that project to the principal signaling center in *Drosophila* imaginal discs. *Cell* 97: 599–607.
35. Sherer NM, Mothes W (2008) Cytosomes and tunneling nanotubes in cell-cell communication and viral pathogenesis. *Trends Cell Biol* 18: 414–420.
36. Roy S, Hsiung F, Kornberg TB (2011) Specificity of *Drosophila* cytosomes for distinct signaling pathways. *Science* 332: 354–358.
37. Somogyi K, Rorth P (2004) Evidence for tension-based regulation of *Drosophila* MAL and SRF during invasive cell migration. *Dev Cell* 7: 85–93.
38. Bogdan S, Grewe O, Strunk M, Mertens A, Klambt C (2004) Sra-1 interacts with Kette and Wasp and is required for neuronal and bristle development in *Drosophila*. *Development* 131: 3981–3989.
39. Mendez-Ferrer S, Michurina TV, Ferraro F, Mazloom AR, Macarthur BD, et al. (2010) Mesenchymal and haematopoietic stem cells form a unique bone marrow niche. *Nature* 466: 829–834.
40. Callejo A, Bilioni A, Mollica E, Gorfinkel N, Andres G, et al. (2011) Dispatched mediates Hedgehog basolateral release to form the long-range morphogenetic gradient in the *Drosophila* wing disk epithelium. *Proc Natl Acad Sci U S A* 108: 12591–12598.
41. Lee JD, Treisman JE (2001) Sightless has homology to transmembrane acyltransferases and is required to generate active Hedgehog protein. *Curr Biol* 11: 1147–1152.
42. Callejo A, Torroja C, Quijada L, Guerrero I (2006) Hedgehog lipid modifications are required for Hedgehog stabilization in the extracellular matrix. *Development* 133: 471–483.
43. Tworzyllo W, Kloc M, Bilinski SM (2010) Female germline stem cell niches of earwigs are structurally simple and different from those of *Drosophila melanogaster*. *J Morphol* 271: 634–640.
44. Crittenden SL, Leonhard KA, Byrd DT, Kimble J (2006) Cellular analyses of the mitotic region in the *Caenorhabditis elegans* adult germ line. *Mol Biol Cell* 17: 3051–3061.
45. Gustavson E, Goldsborough AS, Ali Z, Kornberg TB (1996) The *Drosophila* engrailed and invected genes: partners in regulation, expression and function. *Genetics* 142: 893–906.
46. Lee JJ, von Kessler DP, Parks S, Beachy PA (1992) Secretion and localized transcription suggest a role in positional signaling for products of the segmentation gene hedgehog. *Cell* 71: 33–50.
47. van den Heuvel M, Ingham PW (1996) smoothened encodes a receptor-like serpentine protein required for hedgehog signalling. *Nature* 382: 547–551.
48. Nüsslein-Volhard C, Wieschaus E (1980) Mutations affecting segment number and polarity in *Drosophila*. *Nature* 287: 795–801.
49. Struhl G, Barbash DA, Lawrence PA (1997) Hedgehog organises the pattern and polarity of epidermal cells in the *Drosophila* abdomen. *Development* 124: 2143–2154.
50. Chase BA, Baker BS (1995) A genetic analysis of intersex, a gene regulating sexual differentiation in *Drosophila melanogaster* females. *Genetics* 139: 1649–1661.
51. Bolívar J, Pearson J, López-Onieva L, González-Reyes A (2006) Genetic dissection of a stem cell niche: the case of the *Drosophila* ovary. *Dev Dyn* 235: 2969–2979.
52. Eugster C, Panakova D, Mahmoud A, Eaton S (2007) Lipoprotein-heparan sulfate interactions in the Hh pathway. *Dev Cell* 13: 57–71.
53. Livak KJ, Schmittgen TD (2001) Analysis of relative gene expression data using real-time quantitative PCR and the $2^{-\Delta\Delta C(T)}$ Method. *Methods* 25: 402–408.